

Research Paper

Cortical Morphology in Cannabis Use Disorder: Implications for Transcranial Direct Current Stimulation Treatment



Ghazaleh Soleimani¹, Farzad Towhidkhah^{1*}, Mehrdad Saviz¹, Hamed Ekhtiari²

1. Department of Biomedical Engineering, Faculty of Biomedical Engineering, Amirkabir University of Technology, Tehran, Iran.
2. Laureate Institute of Brain Research, Tulsa, United States of America.



Citation Soleimani, Gh., Towhidkhah, F., Saviz, M., & Ekhtiari, H. (2023). Cortical Morphology in Cannabis Use Disorder: Implications for Transcranial Direct Current Stimulation Treatment. *Basic and Clinical Neuroscience*, 14(5), 647-662. <http://dx.doi.org/10.32598/bcn.2021.3400.1>

doi <http://dx.doi.org/10.32598/bcn.2021.3400.1>



Article info:

Received: 17 May 2021
First Revision: 18 Sep 2021
Accepted: 27 May 2023
Available Online: 01 Sep 2023

Keywords:

tDCS, Individual differences, Cortical morphology, Computational head models, Dorsolateral prefrontal cortex, Substance use disorder

ABSTRACT

Introduction: Transcranial direct current stimulation (tDCS) has been studied as an adjunctive treatment option for substance use disorders (SUDs). Alterations in brain structure following SUD may change tDCS-induced electric field (EF) and subsequent responses; however, group-level differences between healthy controls (HC) and participants with SUDs in terms of EF and its association with cortical architecture have not yet been modeled quantitatively. This study provides a methodology for group-level analysis of computational head models to investigate the influence of cortical morphology metrics on EFs.

Methods: Whole-brain surface-based morphology was conducted, and cortical thickness, volume, and surface area were compared between participants with cannabis use disorders (CUD) (n=20) and age-matched HC (n=22). Meanwhile, EFs were simulated for bilateral tDCS over the dorsolateral prefrontal cortex. The effects of structural alterations on EF distribution were investigated based on individualized computational head models.

Results: Regarding EF, no significant difference was found within the prefrontal cortex; however, EFs were significantly different in left-postcentral and right-superior temporal gyrus (P<0.05) with higher levels of variance in CUD compared to HC [$F_{(39, 43)}=5.31, P<0.0001, C=0.95$]. Significant differences were observed in cortical area (caudal anterior cingulate and rostral middle frontal), thickness (lateral orbitofrontal), and volume (paracentral and fusiform) between the two groups.

Conclusion: Brain morphology and tDCS-induced EFs may be changed following CUD; however, differences between CUD and HCs in EFs do not always overlap with brain areas that show structural alterations. To sufficiently modulate stimulation targets, whether individuals with CUD need different stimulation doses based on tDCS target location should be checked.

* Corresponding Author:

Farzad Towhidkhah, Professor.

Address: Department of Biomedical Engineering, Faculty of Biomedical Engineering, Amirkabir University of Technology, Tehran, Iran.

Tel: +98 (21) 64542363

E-mail: towhidkhah@aut.ac.ir

Highlights

- No electric field electric (EF) difference in prefrontal cortex in cannabis use disorders (CUD) vs healthy controls (HC).
- Varied EFs in postcentral, temporal gyrus in CUD.
- CUD shows altered cortical area, thickness, volume.
- Transcranial direct current stimulation (tDCS) dose adjustments needed for CUD based on EFs.

Plain Language Summary

This study explores how a brain stimulation technique, known as transcranial direct current stimulation (tDCS), affects individuals with cocaine use disorder (CUD) compared to healthy individuals. tDCS is a non-invasive method that uses a low electrical current to stimulate specific parts of the brain. It's being researched as a potential treatment for various brain-related conditions, including substance use disorders. Our research aimed to understand how changes in the brain's structure, often seen in people with substance use disorders, might influence the effects of this brain stimulation. We compared brain scans from 20 individuals with CUD and 22 healthy individuals. These scans helped us look at differences in brain volume, thickness, and surface area. We found that the electrical fields generated by tDCS in the brain were different between the two groups, especially in certain brain areas. Interestingly, these differences did not always line up with the areas where we saw structural changes due to CUD. This suggests that the effects of tDCS are not solely dependent on the structural changes caused by substance use. Why is this important? Our findings indicate that standard tDCS treatment protocols might not be equally effective for individuals with substance use disorders. They may require tailored approaches, considering their unique brain structures. This research is crucial as it paves the way for more personalized and potentially more effective treatments for those struggling with substance use disorders. It also opens up new avenues for understanding how brain stimulation techniques can be optimized based on individual brain characteristics.

1. Introduction

The number of cannabis users has increased in recent years, and despite its legalization in different parts of the world, concerns remain about its effects on adolescents' brains (Connor et al., 2021; Kroon et al., 2020). Although cannabis is one of the most consumed drugs globally, no validated drug treatment is currently available. Available pharmacological therapies for cannabis use disorders (CUD) have low long-term success rates (Fogaça et al., 2013); therefore, there is an urgent need to identify and develop novel therapeutic interventions for CUD. Recent advancements in human neuroscience have provided new adjuvant treatment options, including noninvasive brain stimulation (NIBS) interventions based on targeting the neurocognitive processes of individuals with CUD who desire to quit substance abuse (Kearney-Ramos & Haney, 2021; Sahlem et al., 2020).

In substance use disorders (SUDs), activity in the prefrontal cortex and its connectivity to the subcortical regions (including striatum and amygdala) that are related to addictive behaviors, such as drug craving, can be modulated by NIBS methods (Jansen et al., 2013; Ma et al., 2019). Research on repetitive transcranial magnetic stimulation to treat CUD showed encouraging results for enhancing drug craving or consumption (Kearney-Ramos & Haney, 2021; Martin-Rodriguez et al., 2021; Prashad et al., 2019; Sahlem et al., 2018; Sahlem et al., 2020). Transcranial direct current stimulation (tDCS), a portable and low-cost device, can considerably affect executive functions and addictive behaviors (Chen et al., 2020; Kim & Kang, 2020). For example, previous investigations revealed that tDCS can affect decision-making and cravings in chronic marijuana users (Boggio et al., 2010). The application of tDCS in the field of CUD has attracted more attention in recent years, and two ongoing Clinical Trials registered in 2020 (NCT04389528) and 2021 (NCT04871048) confirm the growing interest in using tDCS as a treatment option for CUD. However, it is unclear whether the dosing parameters used for previ-

ous tDCS studies (among healthy controls or other types of addiction) will be productive in CUD. To use tDCS as a treatment option for CUD, it is critical to consider unique aspects of the neurobiological effects of cannabis that might influence the efficacy of brain stimulation.

Structural cortical abnormalities have consistently been found in people with SUDs and CUD (Chye et al., 2021; Chye et al., 2019; Cousijn et al., 2012; Lorenzetti et al., 2019; Lorenzetti et al., 2020). Various factors (for example, types of drugs, addiction severity, and age of onset) affect the extent and location of morphological changes in the cerebral cortex. Given that tDCS produces diffuse current flow, brain morphological alterations (in targeted or non-targeted brain areas) following CUD can be one of the most critical factors affecting tDCS outcomes. For example, the efficacy of tDCS in prefrontal regions, which is commonly used as a target in brain stimulation studies, is related to underlying cortical morphology (Filmer et al., 2019; Suen et al., 2021). Inspired by McCalley & Hanlon, 2021, brain structural changes in cannabis dependence can affect tDCS-induced electric field distribution patterns that might be associated with further behavioral changes in response to tDCS (Kim et al., 2014; Laakso et al., 2019; Suen et al., 2021). Concerning the brain morphology alterations in CUD and the critical role of the brain structure in the efficacy of tDCS, individuals with CUD may need a different stimulation dose to sufficiently modulate cortical regions compared to age-matched healthy controls without CUD.

In this study, the main goal is to examine the impact of heavy cannabis use on cortical thickness, volume, and surface area in participants with CUD and age-matched healthy controls (HC) in a whole-brain approach and within common cortical tDCS targets in SUDs. Effects of alterations in brain structure on the electric field distribution patterns were also investigated based on individualized computational head models (CHMs). Since participants with CUD may have different cortical structures, we hypothesized that regions with different cortical morphology would differ in electric field distribution patterns. It might need to be applied with different stimulation doses than HC to modulate the brain similarly.

2. Materials and Methods

Study participants

T1-weighted MR images were collected in a separate MRI study (Koenders et al., 2016). The data was obtained from the [OpenfMRI](#) database. This dataset is related to a longitudinal study (T1-weighted structural

MRI study at baseline and three-year follow-up); only the baseline images were used. MRI scans were obtained from two groups of subjects as follows: 22 HC in the age range of 21.6 ± 2.45 years without a history of drug abuse and 20 heavy cannabis users (CB) in the age range of 20.5 ± 2.1 years. Demographic information per group is provided in [Table 1](#).

Analysis pipeline

The workflow for data extraction is illustrated in [Figure 1](#). The analysis method consisted of two parts: 1) Structural data processing and 2) Creation of CHMs. They were both based on the surface-based reconstruction of brain images. The details of data analysis are described in the following sections.

Structural data processing

To analyze the brain structure, T1-weighted MR images were processed using FreeSurfer analysis environment software, version 6.0, freely available online. An automated processing pipeline (“recon-all” with the default set of parameters), which allows surface-based 3-dimensional reconstruction and quantification of cortical morphology, was used to calculate gray matter (GM) volume, surface area, and cortical thickness for each hemisphere. Surface-based processing steps were based on previous reports (Dale et al., 1999; Fischl et al., 1999). The processing steps included motion correction, removal of non-brain tissue, transformation to Talairach space, intensity normalization, segmentation of sub-cortical tissues, intensity normalization, tessellation of the GM-white matter (WM) boundary, automated topology correction, and surface deformation. All reconstructions were visually inspected and manually edited to ensure proper classifications and reconstructions for all subjects. The reconstructed surfaces were registered to a standard surface (“fsaverage”) in the FreeSurfer software with a smoothing level full-width half-maximum Gaussian kernel of 10 mm to allow matching of cortical locations across subjects (Fischl et al., 1999).

Cortical thickness was measured by averaging the distance between the pial surface and the GM-WM surface (Fischl & Dale, 2000). The surface area was computed at the GM-WM boundary as the average area of all triangles surrounding each vertex. Cortical volume was obtained by multiplying cortical area and cortical thickness vertex-by-vertex by the automated procedure for volumetric measures of the brain structures implemented in the FreeSurfer software. Cortical measurements aligned in standard fsaverage space were fed into the general linear

Table 1. Demographic information per group

Variables	Mean±SD/No (%)				
	CB (n=20)	HC (n=22)	Statistic	P	
Gender (male)	75	64	$\chi^2(1)=0.63$	0.43	
Age (y)	20.5±2.11	21.6±2.45	t=1.45	0.15	
CUDIT (y)	12.70±6.59	0.05±0.21	t=9.00	0.001*	
AUDIT	6.25(3.35)	4.41(3.38)	t=1.77	0.08	
Cannabis use	Onset of 1 st use, age (y)	14.50(1.65)	18.46(2.99)	t=4.37	0.001*
	Onset regular use, age (y)	16.29(2.35)	NA	NA	NA
	Current use, grams per week	2.78(1.78)	NA	NA	NA
	Current use, days per week	4.70(1.62)	NA	NA	NA

*P<0.001.

NEURSCIENCE

Abbreviations: CB: Heavy cannabis users; HC: Healthy controls; CB: Cannabis users; HC: Healthy controls.

model using “mri_glmfit” to compare each structural measurement between two groups at each vertex along with the cortical mesh. The statistical maps were thresholded at $P<0.05$ and corrected for multiple comparisons. To assess the spatial overlap of EF and structural measurements (thickness, area, and volume), significant clusters from each whole-brain analysis that survived multiple comparison corrections were combined with EFs in a conjunction map. Finally, automated cortical parcellation and region of interest (ROI) definition were performed using Desikan Killiani atlas (Fan et al., 2016), resulting in mean cortical surface area, cortical thickness, and cortical volume estimations calculated from all vertices within the atlas cortical parcellations per hemisphere.

Creating computational head models

Modeling of induced EFs was performed using the standard SimNIBS 3.0 (Thielscher et al., 2015). In the first step, T1-weighted MR images were segmented into five tissue types: Scalp, skull, cerebrospinal fluid, GM, and WM. The segmentations were carefully examined slice by slice to ensure accurate segmentation of the brain tissues. Then, tetrahedral meshes were generated for each segmented tissue and visualized using Gmsh (Geuzaine & Remacle, 2009). Two large conventional electrode pads (5×7 cm²) with 1 mm thickness were simulated. Anode/cathode electrode was placed over the F3/F4 in an EEG 10-20 standard system with 2 mA current intensity. The dorsolateral prefrontal cortex (DLPFC) is commonly targeted by tDCS or transcranial magnetic stimulation (TMS). In this study, we only focused on the bilateral F4/F3 DLPFC stimula-

tion; according to previous systematic reviews, this montage is the most frequent for people with SUDs (Ekhtiari et al., 2019). However, the pipeline is adaptable to other electrode montages as well. In the next step, linear electrical conductivities (σ) were assigned to each voxel based on the previously reported isotropic values (scalp: 0.465, skull:0.010, CSF: 1.654, GM:0.275, WM: 0.126, electrode rubber sheet: 0.1; all in Siemens/meter).

Subsequently, a transformation was applied to the individualized head models to normalize them into a standard space. To do group-level analysis, the surface-based EFs were mapped into the standard average surface (“fsaverage”) of the FreeSurfer using the inter-subject registration procedure in SimNIBS (Fischl et al., 1999). All head models were fed into the FreeSurfer software, and a general linear model (with “mri_glmfit”) was used to evaluate the main effect of the group on EF. Resultant statistical maps were thresholded at $P<0.05$ and corrected for multiple comparisons. In addition to whole-brain calculations, we applied ROIs analysis based on standard parcellation of CHMs using the Desikan Killiani atlas (Fan et al., 2016). As an indicator of stimulation strength, the spatial mean EF was calculated in all ROIs obtained from atlas-based parcellation.

Association analysis

All statistical analyses were performed in the R statistical software, version 4.3.1 (Team, 2013) and MATLAB software, version 2018b. Atlas-based parcellation extracted cortical measures, mean EF, and peak EF from

each sub-region. Six different linear mixed effect models (LMEs) were used to indicate the relationship between the structural features (surface area, cortical thickness, and cortical volume) and EF indices (2 different measures: Mean and peak). LMEs allow us to investigate the effects of explanatory variables and their interactions (group, ROI, cortical measures as “fixed effects”) on the dependent variable (EF distribution patterns) while statistically controlling for the effects of randomly selected subjects (“random effect”) on the dependent variable. Multiple models were run, and a likelihood-ratio test via the analysis of variance was used to investigate the goodness of fit of different models. Each model was “EF index=group+structural feature+structural feature×group” with a random effect for the subject.

Since this study found no significant role for group or group by structure interaction in LME models, the correlation between induced EFs and structural measurements was calculated separately in all 34 cortical parcellations per hemisphere for each group. For all the statistical analyses in R, false discovery rate correction was used to correct P for ignoring multiple comparisons, and P-corrected <0.05 was considered significant.

3. Results

Extraction of structural characteristic results

The comparison of structural measurements in CB and HC groups is presented in Figure 2 and Table 2. The significant clusters in Table 1 are named based on the Desikan-Killiani atlas annotation in FreeSurfer. CB group showed significantly decreased cortical surface area in the left hemisphere in two clusters. The clusters were in the caudal anterior cingulate and rostral middle frontal.

CB group revealed substantially lower cortical thickness in the right hemisphere in one cluster. The cluster was in the lateral orbitofrontal. Based on cortical volume analysis, the CB group showed significantly lower volume in two clusters, including paracentral and fusiform in the left hemisphere. These significant clusters were considered the main ROIs for comparing induced EFs between the two groups.

Creation of computational head models results

In the second line of our analysis, surface-based CHMs were simulated for all 42 participants (n=22 for the HC group and n=20 for the CB group). At the group-level analysis of CHMs, the Mean±SD of the absolute EFs are shown for each group in Figure 3. Bilateral DLPFC stimulation induced higher EFs in the CB group (global maximum values range from 0.34 to 0.95 V/m) than HC (global maximum values range from 0.34 to 0.59 V/m). Furthermore, the SD of the EF intensity in the CB group was higher than HC, which can indicate higher inter-individual variability among the participants of the CB group.

Figure 3b depicts the results from the whole-brain analysis comparing EFs between the CB group and HC; clusters in this figure are surviving multiple comparison corrections. As mentioned in Table 3, significant clusters were found in the left (CB>HC: Fusiform, temporal pole, supramarginal, lateral occipital, and parahippocampal middle temporal; HC>CB: Superior frontal and postcentral) and right (CB>HC: Lateral occipital, inferior temporal, inferior parietal, middle temporal, parahippocampal, fusiform, inferior parietal, and superior temporal) hemispheres. These significant clusters were considered the main ROIs for finding the correlations

Table 2. Morphological differences between cannabis and healthy groups

Brain Location	Contrast	Cluster Size (mm ²)	CWP	MNI Coordinate			
				x	y	z	
Surface area left hemisphere	Caudal anterior cingulate	HC>CB	3773.63	0.00260	-6.3	15.5	30.7
	Rostral middle frontal	HC>CB	3673.80	0.00320	-31.0	46.1	16.0
Thickness right hemisphere	Lateral orbitofrontal	HC>CB	1379.18	0.01594	33.7	29.2	-15.7
Volume left hemisphere	Paracentral	HC>CB	1635.61	0.00898	-15.5	-43.1	69.2
	Fusiform	HC>CB	1463.91	0.01851	-34.3	-13.7	-31.8

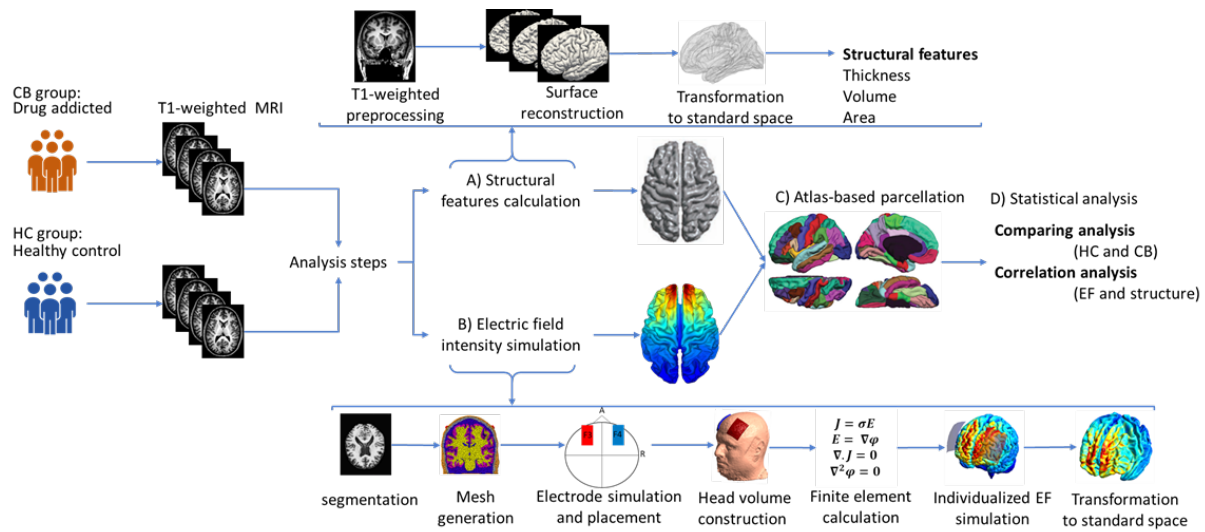


Figure 1. Workflow for data analysis

NEURSCIENCE

Notes: T1-weighted anatomical images were collected in a separate magnetic resonance imaging study from two groups of subjects: Cannabis users (CB group; $n=20$) and healthy controls (HC group; $n=22$). Structural magnetic resonance imaging was analyzed in two separate lines in the next step. A) Extraction of structural characteristics: Structural magnetic resonance imaging was preprocessed in Freesurfer; after surface reconstruction for all of the subjects, each brain surface was transformed to fsaverage standard space, and structural features of the brain, including thickness, volume, and area were calculated at the group-level. The general linear model determined between-group differences regarding cortical morphology metrics; B) Electric field intensity simulations; in the second line of analysis, surface-based computational head models were simulated based on the following steps: Segmentation of the T-weighted images, calculation of the head volume meshes, modeling and placement of two 5×7 cm² electrode pads, simulation of the bilateral transcranial direct current stimulation montage aimed at the dorsolateral prefrontal cortex stimulation (anode/cathode over F3/F4 in EEG 10-20 standard system with 2 mA current intensity), calculation of finite element method, predict electric field intensity distribution for each individual, and transformation of the models to the standard fsaverage space. Similar to structural data, a general linear model was used for group-level analysis of CHMs; C) Atlas-based parcellation: A surface-based anatomical atlas (Desikan-Killiani) was applied to the brain surfaces. The computational head models' structural features and electric field intensity were calculated in each brain region; D) Statistical analysis: Correlation between electric field and cortical metrics was calculated for each individual and group. Linear mixed-effect models were used to investigate the effects of cortical metrics on induced electric fields.

between induced EFs and cortical metrics. The size (in mm²) of each cluster and Montreal Neurological Institute coordinate for the location of maximum significance (z-score) are reported in Table 3. The results are reported based on Freesurfer's automatically labeled parcellation scheme defining temporal, parietal, and occipital cortices separately.

Association results

In five ROIs (paracentral, fusiform, caudal anterior cingulate, rostral middle frontal in the left hemisphere, and lateral orbitofrontal in the right hemisphere) obtained from the morphological analysis (reported in Table 2), the difference between the two groups was calculated in terms of mean EFs. Accordingly, in the left fusiform, the mean EF in the CB group (0.0725 ± 0.01) was significantly ($P=0.0091$) higher than the HC group (0.0662 ± 0.01); however, no significant difference was found in other clusters.

As mentioned in Table 4, LME models showed no main effects of group or group by structure interaction for both mean and peak EFs; however, we found the main effects for all of the structural measurements ($P < 0.001$) in peak EF estimation and the main effect of thickness in mean EF calculations ($P < 0.001$).

After the parcellation of the CHMs based on the Desikan-Killiani atlas, the mean and peak EFs were extracted from each region. The correlation between induced EFs (mean or peak) and each structural characteristic (surface area, cortical thickness, or cortical volume) was also calculated at the ROI level. The calculations showed a significant correlation between mean EF and cortical thickness in the CB group's left superior frontal gyrus ($R=0.7$, $P=0.044$). Nonetheless, we found more significant correlations between brain features and induced EFs in the HC group. Our results demonstrated that the correlations between mean EF and cortical thickness were significant in the left ($R=0.73$, $P=0.008$) and right ($R=0.65$, $P=0.033$) frontal pole. Furthermore, correla-

Table 3. Electric field distribution differences between cannabis and healthy groups

Brain Location	Contrast	Cluster Size (mm ²)	CWP	MNI Coordinate			
				x	y	z	
Left hemisphere	Fusiform	CB>HC	5491.47	0.00020	-32.7	-34.3	-24.7
	Temporal pole	CB>HC	447.92	0.00020	-29.0	9.0	-38.8
	Supramarginal	CB>HC	365.47	0.00140	-53.6	-52.5	23.7
	Lateral occipital	CB>HC	290.04	0.00092	-13.9	-95.3	-12.8
	Para hippocampal	CB>HC	280.70	0.01157	-24.0	-28.5	-22.9
	Middle temporal	CB>HC	243.05	0.03076	-56.4	-22.6	-21.0
	Superior frontal	HC>CB	489.97	0.00020	-6.5	9.3	62.9
	Postcentral	HC>CB	302.92	0.00679	-43.1	-7.8	14.4
	Superior frontal	HC>CB	289.22	0.00918	-8.6	26.9	36.2
Right hemisphere	Lateral occipital	CB>HC	3624.41	0.00020	22.5	-95.8	-12.9
	Inferior temporal	CB>HC	977.74	0.00020	50.5	-36.6	-23.9
	Inferior parietal	CB>HC	604.83	0.00020	40.6	-67.8	26.1
	Middle temporal	CB>HC	591.15	0.00020	49.6	-57.9	1.4
	Para hippocampal	CB>HC	369.51	0.00040	17.8	-37.9	-8.2
	Fusiform	CB>HC	355.97	0.00080	35.0	-3.7	-39.6
	Inferior parietal	CB>HC	315.60	0.00380	48.4	-60.2	25.6
	Superior temporal	CB>HC	292.74	0.00898	46.5	11.0	-22.6

Abbreviations: MNI: Montreal Neurological Institute; HC: Healthy controls; CB: Cannabis users; CWP: Cluster-wise P.

tions between peak EFs and cortical thickness were significant in the left ($R=0.63$, $P=0.042$) and right frontal pole ($R=0.7$, $P=0.018$). The correlation between cortical volume and EFs showed a significant correlation with mean EF in the left frontal pole ($R=0.78$, $P=0.001$) only in the HC group.

4. Discussion

This investigation examining brain morphology and tDCS-induced electric field (EF) differences between healthy controls (HCs) and a group of participants with SUDs yielded four main results. First, the CB group showed a lower surface area in the left caudal anterior cingulate and left rostral middle frontal gyrus, lower cortical thickness in the right lateral orbitofrontal, and lower cortical volume in the paracentral and fusiform gyrus in the left hemisphere. Second, the results showed the greatest mean EF in the frontal pole and the highest maximum

EF in the superior frontal gyrus, with more significant inter-individual variability among heavy cannabis users (CB group) compared to healthy controls (HC group). Third, EF in the fusiform gyrus was significantly different between the two groups. However, no main effects of group and group by structure interaction on induced EFs (mean or peak) were found. Finally, we found that the bilateral DLPFC stimulation frontal pole received the highest EF across the brain, showing significant correlations between induced EFs and brain structure.

Conforming with the previous modeling studies, our simulation results showed inter-individual variability within both HC and CB groups in terms of EF intensity due to individual brain anatomy (Laakso et al., 2015; Laakso et al., 2016; Opitz et al., 2015) with greater SD in CB group (Figure 2). The higher SD among heavy cannabis users can be considered an indirect indicator of more variability in brain structure compared to healthy

Table 4. Results of six linear mixed effects models after applying atlas parcellation to determine the role of group, structural, interaction of group by structure as predictors, subjects as intercept and mean electric field and peak electric field as two separate dependent variables

Predictors	Mean EF			Peak EF			
	Estimates	CI	P	Estimates	CI	P	
Model 1	Intercept	0.13	0.12–0.13	<0.001	0.20	0.18-0.22	<0.001
	Group	-0.00	-0.01-0.01	0.543	-0.01	-0.03-0.02	0.465
	Area	-0.00	-0.02-0.02	0.803	0.11	0.07-0.14	<0.001
	Group×Area	0.01	-0.02-0.03	0.718	-0.03	-0.07-0.02	0.252
Model 2	Intercept	0.12	0.12-0.13	<0.001	0.19	0.17-0.21	<0.001
	Group	-0.00	-0.01-0.01	0.641	-0.01	-0.03-0.02	0.563
	Volume	0.01	-0.00-0.01	0.171	0.05	0.04-0.07	<0.001
	Group×Volume	0.00	-0.01-0.01	0.905	-0.01	-0.03-0.00	0.121
Model 3	Intercept	0.06	0.03-0.08	<0.001	0.12	0.07-0.16	<0.001
	Group	0.01	-0.02-0.04	0.528	0.01	-0.05-0.06	0.864
	Thickness	0.03	0.02-0.04	<0.001	0.04	0.03-0.06	<0.001
	Group×Thickness	-0.00	-0.02-0.01	0.430	-0.01	-0.03-0.01	0.442

CI: Confidence interval; EF, Electric field.

NEURSCIENCE

subjects (Lorenzetti et al., 2019). Populations with SUDs are highly variable from person to person. Different parameters, including clinical characteristics such as the history of polydrug abuse, biological factors such as a person's genetic background, and psychological aspects related to the person's unique history and personality during their lifetime may affect brain alterations resulting from substance use (Abuse et al., 2016). Higher inter-individual variations across participants in the CB group emphasize the importance of individualized treatment plans to tailor tDCS as a therapeutic method in addiction medicine.

Our simulations, in line with previous computational modeling studies, revealed that bilateral electrode montage (Nasseri et al., 2015) could be a suitable electrode configuration to modulate DLPFC. However, given the diffusivity of the brain current flow produced by conventional tDCS and the interaction between different brain regions, it would be challenging to explain causality between a targeted brain region (for instance, DLPFC in this study) and stimulation outcomes (Kuo et al., 2013). For example, in addition to DLPFC, the orbitofrontal cortex (OFC), as a part of the prefrontal cortex, also received high EFs in bilateral stimulation of DLPFC.

OFC is implicated in emotional/motivational executive functions (Fuster, 2001) and has specific connections with subcortical associative learning nodes, such as the basolateral amygdala and nucleus accumbens (Chudasama & Robbins, 2006). OFC contributes to monitoring reward values assigned to different choices, and clinical studies have revealed that this region is involved in disorders and behaviors accompanied by risky decision-making and impulsivity, such as drug addiction (Volkow & Fowler, 2000). A recent functional MRI research, by applying repetitive transcranial magnetic stimulation for nicotine-dependent participants, suggested that the anti-craving effects of DLPFC stimulation might be related to decreased activity in medial OFC and nucleus accumbens (Li et al., 2017). Therefore, the diffusivity of the current and the probability of interaction between targeted and non-targeted regions and whole-brain structural alterations should be considered in interpreting the stimulation outcomes in clinical populations. High definition (Datta et al., 2009; Edwards et al., 2013) or multifocal tDCS targeting (Fischer et al., 2017) deliver a more focal stimulation and avoid spreading the current over non-targeted brain regions; however, they have not yet been used for SUDs.

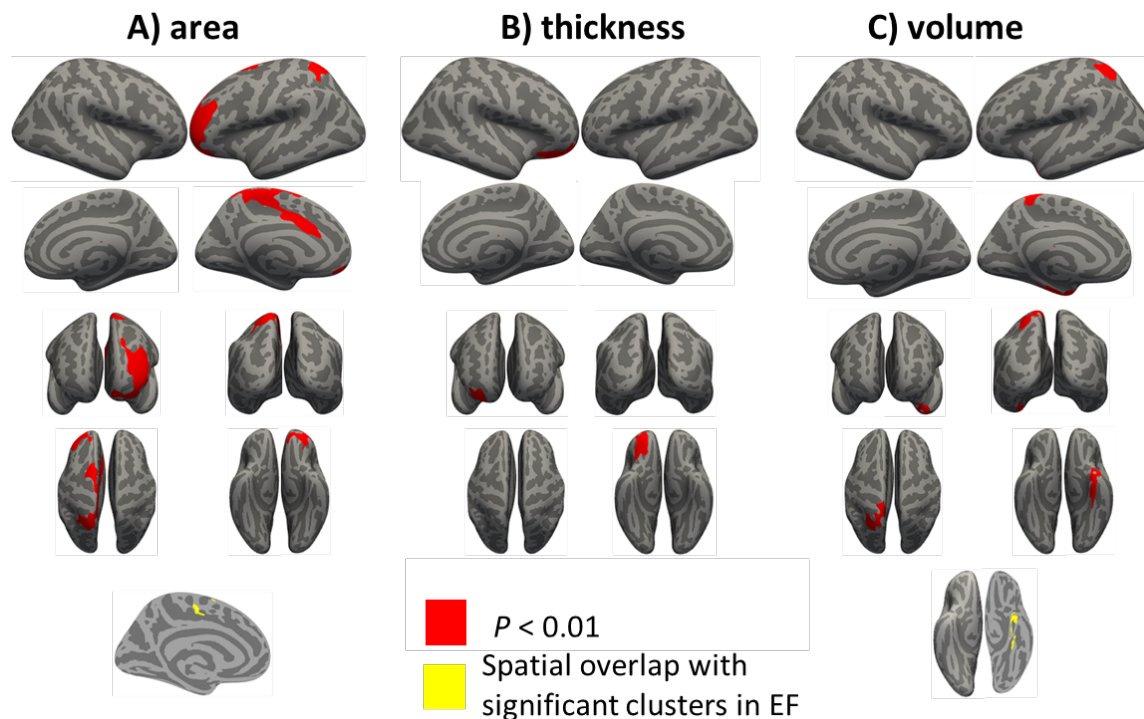


Figure 2. Group-level analysis of cortical measurements

NEUROSCIENCE

A) Surface area, B) Thickness, C) Cortical volume based on a general linear model analysis in Freesurfer

Notes: The results from whole-brain vertex-wise analysis of cortical measurements between cannabis users (CB group) compared with healthy controls (HC group). All of the results are related to HC>CB contrast. Statistical maps are depicted on the inflated surface to allow visualization of sulci (dark gray) and gyri (light gray). Regions that remained significant following a cluster-based multiple comparison correction procedure are depicted (cluster-wise threshold, $P < 0.05$). The lower row is related to the spatial overlap of regions demonstrating significant differences in EFs (illustrated in Figure 3) and significant differences in D) Surface area and E) Cortical volume among the CB group compared with HC

No spatial overlap was found between significant clusters in electric fields and cortical thickness

The whole-brain calculation for comparing two groups of subjects used in this study might be more effective than local comparison in pre-defined ROIs. Whole-brain group-level vertex-wise analysis of CHMs to find between-group differences has not been examined in previous tDCS modeling studies. Consistent with our first hypothesis, the CB group demonstrated different EF intensity than the HC group based on our general linear model approach for CHMS. However, significant clusters obtained from group-level analysis of CHMs were not located in prefrontal cortices as targeted brain areas. Between-group differences in EFs may help explain inconsistent behavioral outcomes since it has been reported that current flow in a cortical target can predict response to tDCS (Datta et al., 2009; Kim et al., 2014; Laakso et al., 2019). For example, different effects of tDCS on cognitive performance in subjects with SUDs compared with healthy controls examined in previously published studies may be related to different EF patterns. For instance, Boggio et al. (2010) reported that anodal stimula-

tion over DLPFC of heavy marijuana users and healthy controls led to increased risk-taking behavior in cannabis users compared with healthy participants; however, the relationship between behavioral outcomes and induced EFs was not investigated. The between-group analysis of CHMs can help find a better answer for between-group variation in the behavioral response to tDCS.

Based on the general linear model analyses of morphological metrics, our results align with previous research. Here, we found a significant difference between CB and HC groups in the right lateral OFC regarding cortical thickness with lower thickness in the CB group. In particular, the right lateral part of the OFC has been implicated in inhibitory processes that suppress previously rewarded choices (Elliott & Deakin, 2005; Elliott et al., 2000). Right lateral OFC produces anticipatory responses about upcoming decisions by integrating prior outcome information with current perceptual details (Nogueira et al., 2017). Levar et al. compared cannabis

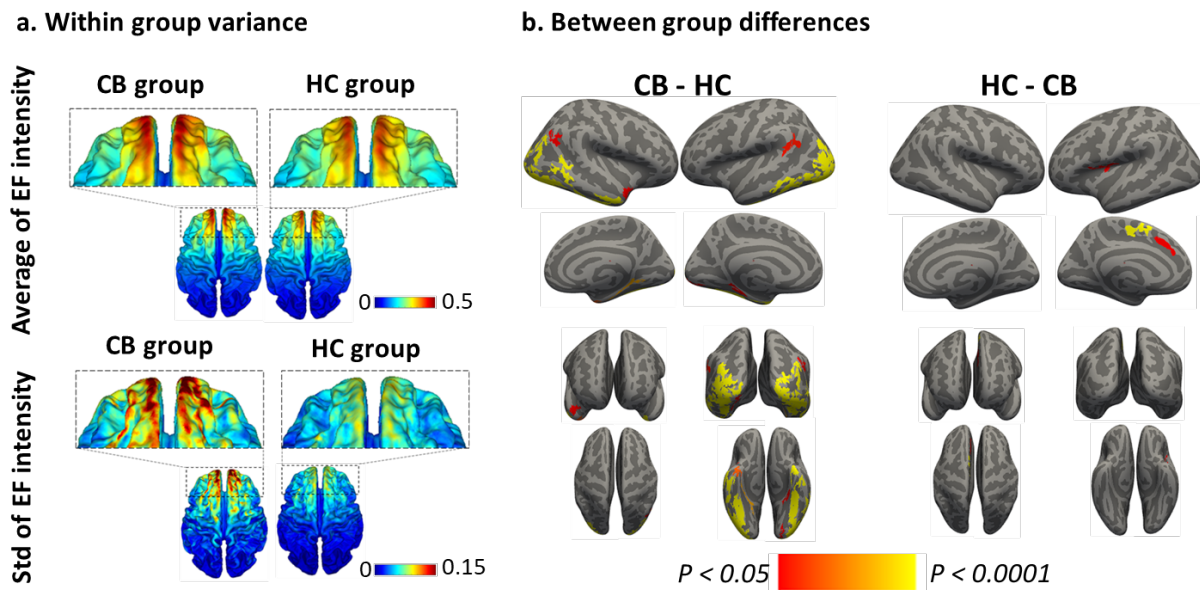


Figure 3a. Within group variance

NEURSCIENCE

Notes: Mean \pm SD of the electric field intensity in volts per meter (V/m) for cannabis users (CB group) and healthy controls (HC group) in standard fsaverage space with bilateral the dorsolateral prefrontal cortex stimulation (anode/cathode over F3/F4 with 2 mA current intensity).

Figure 3b. Between group differences

Notes: The results from whole-brain vertex-wise analysis of electric fields between cannabis users (CB group) compared with healthy controls (HC group) for A) CB>HC and B) HC>CB based on a general linear model analysis in Freesurfer. The statistical maps are depicted on the inflated surface to allow visualization of sulci (dark gray) and gyri (light gray). The regions that remained significant following a cluster-based multiple comparison correction procedure are depicted (cluster-wise threshold, $P < 0.05$).

users with non-users and found a significant main effect of group on the lateral OFC thickness (Levar et al., 2018). In another study, a group of marijuana users was compared with non-user participants. There were some trends toward cortical thickness differences in OFC between groups with lower thickness in marijuana users (Mashhoon et al., 2015). However, there is a lack of consistency in the effects of SUDs on brain structure measurements. For example, no group difference in cortical thickness in CUD (Mata et al., 2010) or thicker cortex in different regions in the frontal, parietal, temporal, and occipital lobe was reported previously on the effects of cannabis use (Jacobus et al., 2015; Lopez-Larson et al., 2011).

Our CB group showed a smaller surface area in the caudal anterior cingulate and rostral middle frontal. These findings are consistent with previous results showing that cannabis use disorder is associated with marginally decreased surface area in the medial and ventral lateral prefrontal cortex (Shollenbarger et al., 2015). A significant cluster was also found in the caudal anterior cingulate when comparing the surface area between

the two groups. The smaller surface area in the caudal anterior cingulate cortex in the CB group may be related to the loss of inhibitory control over the use of cannabis. Yet, our results are inconsistent with prior findings demonstrating no differences between cannabis users and controls (Mata et al., 2010) or significant differences in cuneus surface area (Sullivan et al., 2020). These variations in the effects of SUDs on brain structure in existing literature might be due to some factors, such as the differing number of subjects in previous studies that may affect statistically significant results, age of samples, or analysis design, including whole brain or predefined ROIs analyses.

Here, we found lower cortical volume in the CB group's left paracentral and fusiform gyrus. Few previous studies investigated these brain regions, and marijuana users showed lower density in the parietal lobe and higher density around the fusiform gyrus (Matochik et al., 2005). These regions have been implicated in cognitive processes, particularly attention and working memory (Kirchhoff et al., 2000). They may be related to functional deficits in cannabis users (Bolla et al., 2002).

A previous functional magnetic resonance imaging drug cue-reactivity study reported that specific clusters in occipital, limbic, cerebellum, and temporal regions, including fusiform, activated more during cannabis cues than neutral images. However, fusiform was the only region with a significant negative correlation between activation and craving score. Accordingly, this brain region's role in visual salience might be involved in cue-induced craving (Charboneau et al., 2013).

Despite significant differences in brain structural measurements that we have found between the two groups, we did not find a main effect of group or group by structure (surface area, thickness, or volume) interaction on mean or peak EFs. Hence, induced EFs and distribution of the injected current through the brain were not significantly influenced by structural alterations associated with SUDs. When observing the areas that were significantly different between the two groups in terms of brain structural measurements (including paracentral, fusiform, caudal anterior cingulate, rostral middle frontal in the hemisphere, and lateral OFC in the right hemisphere), we found a subtle difference between two groups in EFs only in the fusiform gyrus. This region is a part of the temporal lobe and is not intentionally targeted in bilateral DLPFC stimulation, and other brain regions showed no significant differences between the two groups. While we found similar patterns of the EF distribution between the two groups, it is still unclear whether this similarity can be interpreted as the same tDCS-related effects in both groups. More functional or behavioral information details are needed to determine differences between the two groups in response to tDCS.

Our findings based on a whole-brain parcellation approach to finding the association between EF and structural measurements in each ROI revealed that correlations between mean/peak EFs and cortical structure were significant in the bilateral frontal pole in the HC group and the left superior frontal gyrus in the CB group. Based on these findings, no significant associations were found in other brain regions. On the other hand, parcellation of CHMs at the group level showed that the frontal pole and superior frontal gyrus were strongly stimulated so that the highest mean and peak EFs were found in these two regions. Therefore, by increasing induced EF intensity, the importance of brain structure will be increased. Our findings suggest that EFs are associated with brain structural measurements such as thickness or volume in strongly stimulated brain areas. Structural differences between the two groups should be considered, especially in these brain regions.

Considerations and future directions

We are aware that our research may have several limitations. Firstly, our results are restricted to structural information of the brain. Behavioral or functional effects of tDCS were not available in our dataset, and we could not assess the relationship between EF intensity, brain structure, and clinical or functional responses to tDCS. However, there is tremendous consensus across the labs on tDCS modeling workflow with key features set since 2009 (Datta et al., 2009). Modeling studies were validated repeatedly in previous in-vivo, in-vitro, and in-silico studies based on human or animal brains. For example, intracranial recordings of brain current flow from 10 living subjects were correlated with subject-specific current flow models (Huang et al., 2017). Independently, intracranial recordings from patients, cadavers, and non-human primates confirm insights from computational healing models (Opitz et al., 2016; Underwood, 2016). Significant engineering effort has been directed toward finite element modeling, and it has been reported that these models can accurately predict the distinct voltage distribution over the scalp, which is correlated with the current flow through the cortex (Datta et al., 2013). Different imaging techniques were also used to detect magnetic fields induced by tDCS currents in post-mortem individuals (Antal et al., 2014) or healthy subjects (Jog et al., 2016). Regarding the validity of head models, CHMs are commonly used to individualize stimulation dose account for vulnerable populations (Kessler et al., 2013; Shekhawat & Vanneste, 2018; Truong et al., 2013).

Next, we used automatic tissue segmentation, and outcomes strongly depend on the quality of the T1-weighted images and segmentation algorithm. More precise segmentation algorithms, especially for creating the head models, can be investigated in future studies. Furthermore, our dataset did not enable evaluating diffusion tensor imaging to consider tissue anisotropy. We have assumed isotropic conductivity, as is common in computational modeling studies. Using previously established electrical conductivity might affect EF distribution patterns, especially in the skull and WM (Opitz et al., 2011; Suh et al., 2012). However, anisotropic conductivity is necessary when EF in deeper parts of the brain is considered (Wagner et al., 2013). Another limitation is that our simulations are focused on EF intensity induced by conventional bilateral tDCS over DLPFC. We ignored the radial component of the EF, which is informative of EF direction. The normal component of the EF reflects current either entering (anodal effect) or leaving the cortex (cathodal effect), which may be instructive in between-group comparisons.

There are still many questions to be answered in future studies. One of the main remaining questions is whether induced EFs in targeted or non-targeted brain areas are associated with other neuroimaging information, such as functional magnetic resonance imaging data. Future research is needed to incorporate head models and fMRI data more comprehensively to help design tES-functional magnetic resonance imaging protocols more accurately, especially in clinical applications. Our pipeline can be used to integrate CHMs with additional neuroimaging information and behavioral outcomes that may shed new light on the sources within/between-group variation in response to tDCS in future works. Furthermore, fundamental questions remain regarding the optimal electrode configuration. Concerning the importance of individualizing stimulation protocols, more simulations are needed to determine personalized electrode montage based on a person's cortical morphology. For example, the ideal montage for subjects with SUDs should be based on a patient-tailored approach that considers different aspects related to alterations in brain structure, and the clinical implications of these montages should be explored in future studies.

5. Conclusion

To the best of our knowledge, this is the first study that compares cannabis users with healthy controls for the implications of tDCS treatment in a whole-brain approach. The results from this study reveal the following items: 1) CUD-induced morphological changes may occur in brain regions relevant to tDCS targets (such as the orbitofrontal cortex); 2) Group-level differences in EF distribution patterns in bilateral stimulation of DLPFC can be found in some non-targeted areas (far from DLPFC as the main target); 3) Group-level differences between CUD and HCs in terms of tDCS-induced EFs do not always overlap with the brain areas obtained from group-level differences in the structural measures; 4) More variance and less significant correlations were found between EF and cortical metrics in cannabis group compared to healthy subjects that emphasize more inter-individual variability among clinical populations. The proposed pipeline in this study can be used to integrate CHMs with other neuroimaging information, including functional MRI data. Pursuing this direction while accounting for cortical morphology and other possible confounding such as functional brain activity, neuropsychiatric background, and so on provides insights into the mechanisms behind inter-individual variability in response to non-invasive brain stimulation technologies.

Ethical Considerations

Compliance with ethical guidelines

There were no ethical considerations to be considered in this research.

Funding

This research did not receive any grant from funding agencies in the public, commercial, or non-profit sectors.

Authors' contributions

Study design: Ghazaleh Soleimani and Hamed Ekhtiari; Data collection: Hamed Ekhtiari, Mehrdad Saviz and Farzad Towhidkhan; Data analysis: Hamed Ekhtiari and Farzad Towhidkhan; Simulations: Ghazaleh Soleimani; Writing paper: Ghazaleh Soleimani; Data interpretation and final approval: All authors.

Conflict of interest

The authors declared no conflict of interest.

References

- Abuse, S., US, M. H. S. A., & General, O. o. t. S. (2016). The neurobiology of substance use, misuse, and addiction. In: *Facing addiction in America: The surgeon general's report on alcohol, drugs, and health*. Washington (DC): US Department of Health and Human Services. [\[Link\]](#)
- Antal, A., Bikson, M., Datta, A., Lafon, B., Dechent, P., & Parra, L. C., et al. (2014). Imaging artifacts induced by electrical stimulation during conventional fMRI of the brain. *NeuroImage*, *85 Pt 3*(0 3), 1040–1047. [\[DOI:10.1016/j.neuroimage.2012.10.026\]](#)
- Boggio, P. S., Zaghi, S., Villani, A. B., Fecteau, S., Pascual-Leone, A., & Fregni, F. (2010). Modulation of risk-taking in marijuana users by transcranial direct current stimulation (tDCS) of the dorsolateral prefrontal cortex (DLPFC). *Drug and Alcohol Dependence*, *112*(3), 220–225. [\[DOI:10.1016/j.drugalcdep.2010.06.019\]](#)
- Bolla, K. I., Brown, K., Eldreth, D., Tate, K., & Cadet, J. L. (2002). Dose-related neurocognitive effects of marijuana use. *Neurology*, *59*(9), 1337–1343. [\[DOI:10.1212/01.WNL.0000031422.66442.49\]](#)
- Charboneau, E. J., Dietrich, M. S., Park, S., Cao, A., Watkins, T. J., & Blackford, J. U., et al. (2013). Cannabis cue-induced brain activation correlates with drug craving in limbic and visual salience regions: Preliminary results. *Psychiatry Research*, *214*(2), 122–131. [\[DOI:10.1016/j.psychres.2013.06.005\]](#)

- Chen, J., Qin, J., He, Q., & Zou, Z. (2020). A meta-analysis of transcranial direct current stimulation on substance and food craving: What effect do modulators have? *Frontiers in Psychiatry*, 11, 598. [DOI:10.3389/fpsyt.2020.00598]
- Chudasama, Y., & Robbins, T. W. (2006). Functions of frontostriatal systems in cognition: Comparative neuropsychopharmacological studies in rats, monkeys and humans. *Biological Psychiatry*, 73(1), 19-38. [DOI:10.1016/j.biopsych.2006.01.005]
- Chye, Y., Kirkham, R., Lorenzetti, V., McTavish, E., Solowij, N., & Yücel, M. (2021). Cannabis, cannabinoids, and brain morphology: A review of the evidence. *Biological Psychiatry, Cognitive Neuroscience and Neuroimaging*, 6(6), 627-635. [DOI:10.1016/j.bpsc.2020.07.009]
- Chye, Y., Lorenzetti, V., Suo, C., Batalla, A., Cousijn, J., & Goudriaan, A. E., et al. (2019). Alteration to hippocampal volume and shape confined to cannabis dependence: A multi-site study. *Addiction Biology*, 24(4), 822-834. [DOI:10.1111/adb.12652]
- Connor, J. P., Stjepanović, D., Le Foll, B., Hoch, E., Budney, A. J., & Hall, W. D. (2021). Cannabis use and cannabis use disorder. *Nature Reviews. Disease Primers*, 7(1), 16. [DOI:10.1038/s41572-021-00247-4]
- Cousijn, J., Wiers, R. W., Ridderinkhof, K. R., van den Brink, W., Veltman, D. J., & Goudriaan, A. E. (2012). Grey matter alterations associated with cannabis use: Results of a VBM study in heavy cannabis users and healthy controls. *Neuroimage*, 59(4), 3845-3851. [DOI:10.1016/j.neuroimage.2011.09.046]
- Dale, A. M., Fischl, B., & Sereno, M. I. (1999). Cortical surface-based analysis. I. Segmentation and surface reconstruction. *Neuroimage*, 9(2), 179-194. [DOI:10.1006/nimg.1998.0395]
- Datta, A., Bansal, V., Diaz, J., Patel, J., Reato, D., & Bikson, M. (2009). Gyri-precise head model of transcranial direct current stimulation: Improved spatial focality using a ring electrode versus conventional rectangular pad. *Brain Stimulation*, 2(4), 201-207.e1. [DOI:10.1016/j.brs.2009.03.005]
- Datta, A., Zhou, X., Su, Y., Parra, L. C., & Bikson, M. (2013). Validation of finite element model of transcranial electrical stimulation using scalp potentials: Implications for clinical dose. *Journal of Neural Engineering*, 10(3), 036018. [DOI:10.1088/1741-2560/10/3/036018]
- Edwards, D., Cortes, M., Datta, A., Minhas, P., Wassermann, E. M., & Bikson, M. (2013). Physiological and modeling evidence for focal transcranial electrical brain stimulation in humans: a basis for high-definition tDCS. *Neuroimage*, 74, 266-275. [DOI:10.1016/j.neuroimage.2013.01.042]
- Ekhtiari, H., Tavakoli, H., Addolorato, G., Baeken, C., Bonci, A., & Campanella, S., et al. (2019). Transcranial electrical and magnetic stimulation (tES and TMS) for addiction medicine: A consensus paper on the present state of the science and the road ahead. *Neuroscience and Biobehavioral Reviews*, 104, 118-140. [DOI:10.1016/j.neubiorev.2019.06.007]
- Elliott, R., & Deakin, B. (2005). Role of the orbitofrontal cortex in reinforcement processing and inhibitory control: Evidence from functional magnetic resonance imaging studies in healthy human subjects. *International Review of Neurobiology*, 65, 89-116. [DOI:10.1016/S0074-7742(04)65004-5]
- Elliott, R., Dolan, R. J., & Frith, C. D. (2000). Dissociable functions in the medial and lateral orbitofrontal cortex: Evidence from human neuroimaging studies. *Cerebral Cortex*, 10(3), 308-317. [DOI:10.1093/cercor/10.3.308]
- Fan, L., Li, H., Zhuo, J., Zhang, Y., Wang, J., & Chen, L., et al. (2016). The human brainnetome atlas: A new brain atlas based on connective architecture. *Cerebral Cortex*, 26(8), 3508-3526. [DOI:10.1093/cercor/bhw157]
- Filmer, H. L., Ehrhardt, S. E., Shaw, T. B., Mattingley, J. B., & Dux, P. E. (2019). The efficacy of transcranial direct current stimulation to prefrontal areas is related to underlying cortical morphology. *Neuroimage*, 196, 41-48. [DOI:10.1016/j.neuroimage.2019.04.026]
- Fischer, D. B., Fried, P. J., Ruffini, G., Ripolles, O., Salvador, R., & Banus, J., et al. (2017). Multifocal tDCS targeting the resting state motor network increases cortical excitability beyond traditional tDCS targeting unilateral motor cortex. *Neuroimage*, 157, 34-44. [DOI:10.1016/j.neuroimage.2017.05.060]
- Fischl, B., & Dale, A. M. (2000). Measuring the thickness of the human cerebral cortex from magnetic resonance images. *Proceedings of the National Academy of Sciences of the United States of America*, 97(20), 11050-11055. [DOI:10.1073/pnas.200033797]
- Fischl, B., Sereno, M. I., & Dale, A. M. (1999). Cortical surface-based analysis: II: Inflation, flattening, and a surface-based coordinate system. *Neuroimage*, 9(2), 195-207. [DOI:10.1006/nimg.1998.0396]
- Fogaça, M. V., Galve-Roperh, I., Guimarães, F. S., & Campos, A. C. (2013). Cannabinoids, neurogenesis and antidepressant drugs: Is there a link? *Current Neuropharmacology*, 11(3), 263-275. [DOI:10.2174/1570159X11311030003]
- Fuster, J. M. (2001). The prefrontal cortex-an update: Time is of the essence. *Neuron*, 30(2), 319-333. [DOI:10.1016/S0896-6273(01)00285-9]
- Geuzaine, C., & Remacle, J. F. (2009). Gmsh: A 3-D finite element mesh generator with built-in pre- and post-processing facilities. *International Journal for Numerical Methods in Engineering*, 79(11), 1309-1331. [DOI:10.1002/nme.2579]
- Huang, Y., Liu, A. A., Lafon, B., Friedman, D., Dayan, M., & Wang, X., et al. (2017). Measurements and models of electric fields in the in vivo human brain during transcranial electric stimulation. *Elife*, 6, e18834. [DOI:10.7554/eLife.18834]
- Jacobus, J., Squeglia, L. M., Meruelo, A. D., Castro, N., Brumback, T., & Giedd, J. N., et al. (2015). Cortical thickness in adolescent marijuana and alcohol users: A three-year prospective study from adolescence to young adulthood. *Developmental Cognitive Neuroscience*, 16, 101-109. [DOI:10.1016/j.dcn.2015.04.006]
- Jansen, J. M., Daams, J. G., Koeter, M. W., Veltman, D. J., van den Brink, W., & Goudriaan, A. E. (2013). Effects of non-invasive neurostimulation on craving: A meta-analysis. *Neuroscience & Biobehavioral Reviews*, 37(10), 2472-2480. [DOI:10.1016/j.neubiorev.2013.07.009]
- Jog, M. V., Smith, R. X., Jann, K., Dunn, W., Lafon, B., & Truong, D., et al. (2016). In-vivo imaging of magnetic fields induced by transcranial direct current stimulation (tDCS) in human brain using MRI. *Scientific Reports*, 6, 34385. [DOI:10.1038/srep34385]
- Kearney-Ramos, T., & Haney, M. (2021). Repetitive transcranial magnetic stimulation as a potential treatment approach for cannabis use disorder. *Progress in Neuro-Psychopharmacology & Biological Psychiatry*, 109, 110290. [DOI:10.1016/j.pnpbp.2021.110290]

- Kessler, S. K., Minhas, P., Woods, A. J., Rosen, A., Gorman, C., & Bikson, M. (2013). Dosage considerations for transcranial direct current stimulation in children: A computational modeling study. *Plos One*, 8(9), e76112. [DOI:10.1371/journal.pone.0076112]
- Kim, H. J., & Kang, N. (2021). Bilateral transcranial direct current stimulation attenuated symptoms of alcohol use disorder: A systematic review and meta-analysis. *Progress in Neuro-Psychopharmacology & Biological Psychiatry*, 108, 110160. [DOI:10.1016/j.pnpbp.2020.110160]
- Kim, J. H., Kim, D. W., Chang, W. H., Kim, Y. H., Kim, K., & Im, C. H. (2014). Inconsistent outcomes of transcranial direct current stimulation may originate from anatomical differences among individuals: Electric field simulation using individual MRI data. *Neuroscience Letters*, 564, 6-10. [DOI:10.1016/j.neulet.2014.01.054]
- Kirchhoff, B. A., Wagner, A. D., Maril, A., & Stern, C. E. (2000). Prefrontal-temporal circuitry for episodic encoding and subsequent memory. *The Journal of Neuroscience: The Official Journal of the Society for Neuroscience*, 20(16), 6173-6180. [DOI:10.1523/JNEUROSCI.20-16-06173.2000]
- Koenders, L., Cousijn, J., Vingerhoets, W. A., van den Brink, W., Wiers, R. W., & Meijer, C. J., et al. (2016). Grey matter changes associated with heavy cannabis use: A longitudinal sMRI study. *PloS One*, 11(5), e0152482. [DOI:10.1371/journal.pone.0152482]
- Kroon, E., Kuhns, L., Hoch, E., & Cousijn, J. (2020). Heavy cannabis use, dependence and the brain: A clinical perspective. *Addiction*, 115(3), 559-572. [DOI:10.1111/add.14776]
- Kuo, H. I., Bikson, M., Datta, A., Minhas, P., Paulus, W., & Kuo, M. F., et al. (2013). Comparing cortical plasticity induced by conventional and high-definition 4x 1 ring tDCS: A neurophysiological study. *Brain Stimulation*, 6(4), 644-648. [DOI:10.1016/j.brs.2012.09.010]
- Laakso, I., Mikkonen, M., Koyama, S., Hirata, A., & Tanaka, S. (2019). Can electric fields explain inter-individual variability in transcranial direct current stimulation of the motor cortex? *Scientific Reports*, 9(1), 626. [DOI:10.1038/s41598-018-37226-x]
- Laakso, I., Tanaka, S., Koyama, S., De Santis, V., & Hirata, A. (2015). Inter-subject variability in electric fields of motor cortical tDCS. *Brain Stimulation*, 8(5), 906-913. [DOI:10.1016/j.brs.2015.05.002]
- Laakso, I., Tanaka, S., Mikkonen, M., Koyama, S., Sadato, N., & Hirata, A. (2016). Electric fields of motor and frontal tDCS in a standard brain space: A computer simulation study. *Neuroimage*, 137, 140-151. [DOI:10.1016/j.neuroimage.2016.05.032]
- Levar, N., Francis, A. N., Smith, M. J., Ho, W. C., & Gilman, J. M. (2018). Verbal memory performance and reduced cortical thickness of brain regions along the uncinate fasciculus in young adult cannabis users. *Cannabis and Cannabinoid Research*, 3(1), 56-65. [DOI:10.1089/can.2017.0030]
- Li, X., Sahlem, G. L., Badran, B. W., McTeague, L. M., Hanlon, C. A., & Hartwell, K. J., et al. (2017). Transcranial magnetic stimulation of the dorsal lateral prefrontal cortex inhibits medial orbitofrontal activity in smokers. *The American Journal on Addictions*, 26(8), 788-794. [DOI:10.1111/ajad.12621]
- Lopez-Larson, M. P., Bogorodzki, P., Rogowska, J., McGlade, E., King, J. B., & Terry, J., et al. (2011). Altered prefrontal and insular cortical thickness in adolescent marijuana users. *Behavioural Brain Research*, 220(1), 164-172. [DOI:10.1016/j.bbr.2011.02.001]
- Lorenzetti, V., Chye, Y., Silva, P., Solowij, N., & Roberts, C. A. (2019). Does regular cannabis use affect neuroanatomy? An updated systematic review and meta-analysis of structural neuroimaging studies. *European Archives of Psychiatry and Clinical Neuroscience*, 269(1), 59-71. [DOI:10.1007/s00406-019-00979-1]
- Lorenzetti, V., Chye, Y., Suo, C., Walterfang, M., Lubman, D. I., & Takagi, M., et al. (2020). Neuroanatomical alterations in people with high and low cannabis dependence. *The Australian and New Zealand journal of psychiatry*, 54(1), 68-75. [DOI:10.1177/0004867419859077]
- Ma, T., Sun, Y., & Ku, Y. (2019). Effects of non-invasive brain stimulation on stimulant craving in users of cocaine, amphetamine, or methamphetamine: A systematic review and meta-analysis. *Frontiers in Neuroscience*, 13, 1095. [DOI:10.3389/fnins.2019.01095]
- Martin-Rodriguez, J. F., Ruiz-Veguilla, M., Alvarez de Toledo, P., Aizpurua-Olaizola, O., Zarandona, L., & Canal-Rivero, M., et al. (2021). Impaired motor cortical plasticity associated with cannabis use disorder in young adults. *Addiction Biology*, 26(3), e12912. [DOI:10.1111/adb.12912]
- Mashhoon, Y., Sava, S., Sneider, J. T., Nickerson, L. D., & Silveri, M. M. (2015). Cortical thinness and volume differences associated with marijuana abuse in emerging adults. *Drug and Alcohol Dependence*, 155, 275-283. [DOI:10.1016/j.drugalcdep.2015.06.016]
- Mata, I., Perez-Iglesias, R., Roiz-Santiañez, R., Tordesillas-Gutierrez, D., Pazos, A., & Gutierrez, A., et al. (2010). Gyri-fication brain abnormalities associated with adolescence and early-adulthood cannabis use. *Brain Research*, 1317, 297-304. [DOI:10.1016/j.brainres.2009.12.069]
- Matochik, J. A., Eldreth, D. A., Cadet, J. L., & Bolla, K. I. (2005). Altered brain tissue composition in heavy marijuana users. *Drug and Alcohol Dependence*, 77(1), 23-30. [DOI:10.1016/j.drugalcdep.2004.06.011]
- McCalley, D. M., & Hanlon, C. A. (2021). Regionally specific gray matter volume decreases in Alcohol Use Disorder: Implications for non-invasive brain stimulation treatment: Implications for non-invasive brain stimulation treatment. *Alcoholism: Clinical and Experimental Research*, 45(8), 1672-1683. [Link]
- Nasseri, P., Nitsche, M. A., & Ekhtiari, H. (2015). A framework for categorizing electrode montages in transcranial direct current stimulation. *Frontiers in Human Neuroscience*, 9, 54. [DOI:10.3389/fnhum.2015.00054]
- Nogueira, R., Abolafia, J. M., Drugowitsch, J., Balaguer-Ballester, E., Sanchez-Vives, M. V., & Moreno-Bote, R. (2017). Lateral orbitofrontal cortex anticipates choices and integrates prior with current information. *Nature Communications*, 8, 14823. [DOI:10.1038/ncomms14823]
- Opitz, A., Falchier, A., Yan, C. G., Yeagle, E. M., Linn, G. S., & Megevand, P., et al. (2016). Spatiotemporal structure of intracranial electric fields induced by transcranial electric stimulation in humans and nonhuman primates. *Scientific Reports*, 6, 31236. [DOI:10.1038/srep31236]
- Opitz, A., Paulus, W., Will, S., Antunes, A., & Thielscher, A. (2015). Determinants of the electric field during transcranial

- nial direct current stimulation. *Neuroimage*, 109, 140-150. [DOI:10.1016/j.neuroimage.2015.01.033]
- Opitz, A., Windhoff, M., Heidemann, R. M., Turner, R., & Thielscher, A. (2011). How the brain tissue shapes the electric field induced by transcranial magnetic stimulation. *Neuroimage*, 58(3), 849-859. [DOI:10.1016/j.neuroimage.2011.06.069]
- Prashad, S., Dedrick, E. S., To, W. T., Vanneste, S., & Filbey, F. M. (2019). Testing the role of the posterior cingulate cortex in processing salient stimuli in cannabis users: An rTMS study. *The European Journal of Neuroscience*, 50(3), 2357-2369. [DOI:10.1111/ejn.14194]
- Sahlem, G. L., Baker, N. L., George, M. S., Malcolm, R. J., & McRae-Clark, A. L. (2018). Repetitive transcranial magnetic stimulation (rTMS) administration to heavy cannabis users. *The American Journal of Drug and Alcohol Abuse*, 44(1), 47-55. [DOI:10.1080/00952990.2017.1355920]
- Sahlem, G. L., Caruso, M. A., Short, E. B., Fox, J. B., Sherman, B. J., & Manett, A. J., et al. (2020). A case series exploring the effect of twenty sessions of repetitive transcranial magnetic stimulation (rTMS) on cannabis use and craving. *Brain Stimulation*, 13(1), 265-266. [DOI:10.1016/j.brs.2019.09.014]
- Shekhawat, G. S., & Vanneste, S. (2018). Optimization of transcranial direct current stimulation of dorsolateral prefrontal cortex for tinnitus: A non-linear dose-response effect. *Scientific Reports*, 8(1), 8311. [DOI:10.1038/s41598-018-26665-1]
- Shollenbarger, S. G., Price, J., Wieser, J., & Lisdahl, K. (2015). Impact of cannabis use on prefrontal and parietal cortex gyrification and surface area in adolescents and emerging adults. *Developmental Cognitive Neuroscience*, 16, 46-53. [DOI:10.1016/j.dcn.2015.07.004]
- Suen, P. J. C., Doll, S., Batistuzzo, M. C., Busatto, G., Razza, L. B., & Padberg, F., et al. (2021). Association between tDCS computational modeling and clinical outcomes in depression: data from the ELECT-TDCS trial. *European Archives of Psychiatry and Clinical Neuroscience*, 271(1), 101-110. [DOI:10.1007/s00406-020-01127-w]
- Suh, H. S., Lee, W. H., & Kim, T. S. (2012). Influence of anisotropic conductivity in the skull and white matter on transcranial direct current stimulation via an anatomically realistic finite element head model. *Physics in Medicine & Biology*, 57(21), 6961-6980. [DOI:10.1088/0031-9155/57/21/6961]
- Sullivan, R. M., Wallace, A. L., Wade, N. E., Swartz, A. M., & Lisdahl, K. M. (2020). Assessing the role of cannabis use on cortical surface structure in adolescents and young adults: Exploring gender and aerobic fitness as potential moderators. *Brain Sciences*, 10(2), 117. [DOI:10.3390/brainsci10020117]
- Team, R. (2021). RStudio: integrated development for R; RStudio, PBC: Boston, MA. 2020. [Link]
- Thielscher, A., Antunes, A., & Saturnino, G. B. (2015). Field modeling for transcranial magnetic stimulation: A useful tool to understand the physiological effects of TMS? *Annual International Conference of the IEEE Engineering in Medicine and Biology Society. IEEE Engineering in Medicine and Biology Society. Annual International Conference, 2015*, 222-225. [DOI:10.1109/EMBC.2015.7318340]
- TTruong, D. Q., Magerowski, G., Blackburn, G. L., Bikson, M., & Alonso-Alonso, M. (2013). Computational modeling of transcranial direct current stimulation (tDCS) in obesity: Impact of head fat and dose guidelines. *NeuroImage. Clinical*, 2, 759-766. [DOI:10.1016/j.nicl.2013.05.011]
- Underwood, E. (2016). Cadaver study casts doubts on how zapping brain may boost mood, relieve pain. Retrieve from: [Link]
- Volkow, N. D., & Fowler, J. S. (2000). Addiction, a disease of compulsion and drive: involvement of the orbitofrontal cortex. *Cerebral Cortex*, 10(3), 318-325. [DOI:10.1093/cercor/10.3.318]
- Wagner, S., Rampersad, S. M., Aydin, Ü., Vorwerk, J., Oostendorp, T. F., & Neuling, T., et al. (2014). Investigation of tDCS volume conduction effects in a highly realistic head model. *Journal of Neural Engineering*, 11(1), 016002. [DOI:10.1088/1741-2560/11/1/016002]

This Page Intentionally Left Blank